Journal of Wind Engineering & Industrial Aerodynamics 273 (2026) 106436

Contents lists available at ScienceDirect

Journal of Wind Engineering & Industrial Aerodynamics

journal homepage: www.elsevier.com/locate/jweia

Experimental assessment of the long-term variation of modal properties and aerodynamic damping of a self-supporting lattice tower

Mekdes T. Mengistu [a,*], Kristof Maes [b], Ileana Calotescu [c], Geert Lombaert [b], Maria Pia Repetto [a]

[a] University of Genova, Genova, Italy
[b] KU Leuven, Leuven, Belgium
[c] Technical University of Civil Engineering Bucharest, Bucharest, Romania

ARTICLE INFO

Keywords:
Lattice tower
Full-scale monitoring
Operational modal analysis
Aerodynamic damping

ABSTRACT

The dynamic properties of a 50 m tall self-supporting lattice tower are investigated using long-term full-scale monitoring. Two years of acceleration, strain, temperature, and wind speed data are analyzed to obtain the natural frequencies, mode shapes, and damping ratios. The environmental variation of the modal characteristics and aerodynamic damping was studied based on the simultaneously recorded temperature and wind data. Natural frequencies decreased with an increase in outside temperature. The damping ratios of the first four modes ranged from about 0.2% at low wind speed to 0.6% at high wind speeds. A clear increase in the damping ratio with the mean wind speed, by more than double, was found for the first four modes. The increasing trend of the damping ratio in the alongwind direction with the wind speed was closely similar to that obtained using the quasi-steady-based formulation. The results of the study are an important addition to the few available studies investigating the dynamic properties of self-supporting lattice towers using full-scale data, which in turn will be an input to design standards.

1. Introduction

Self-supporting lattice towers are crucial infrastructure elements that support electrical transmission lines, lighting systems, communication antennas, and other components. These structures are usually light and slender, making them susceptible to wind-induced dynamic vibration. The design of lattice towers against wind usually follows the gust-factor approach using their geometric and dynamic properties as input (Calotescu and Solari, 2016). In the preliminary design stage, the dynamic properties of lattice structures, including the fundamental frequency and damping ratio, are usually taken from design standards, but in the detailed design stage, it is customary to prepare a finite element model to obtain the natural frequencies and mode shapes. Erroneous assumptions of the dynamic properties might lead to an underestimation or overestimation of the wind-induced dynamic load, affecting the safety or economic aspects of the design.

The dynamic properties of lattice towers have not been extensively investigated through full-scale monitoring. A limited number of studies have reported these properties based on forced or ambient vibration measurements conducted on full-scale structures. The main focus of these studies was to investigate the wind-induced dynamic response of lattice towers through full-scale monitoring, by comparing the measured accelerations and deflections with those predicted using the gust factor approach (Haritos and Stevens, 1983; Hiramatsu and Akagi, 1988; Holmes et al., 1992; Augusti et al., 1992; Shanmugasundaram et al., 1999; Huang et al., 2019; Peng et al., 2017). The results mainly reported the first bending mode, along with its corresponding natural frequency and damping ratio.

Damping is a mechanism by which a vibrating structure dissipates energy, and it arises from multiple sources. For wind-excited structures, in addition to the inherent structural damping, aerodynamic damping occurs as a function of the vibration velocity. Aerodynamic damping might have a positive or a negative effect on the overall dynamic excitation. Using quasi-steady theory, it can be shown that aerodynamic damping results in additional dissipation in the alongwind direction, while it might result in possible instability in the crosswind and torsional directions (Kareem, 1978). For slender and lightweight structures, aerodynamic damping can greatly exceed structural damping.

Although the damping ratio is a key parameter for the dynamic response of slender structures such as lattice towers, its investigation

* Corresponding author.
E-mail addresses: mekdestadesse.mengistu@edu.unige.it (M.T. Mengistu), kristof.maes@kuleuven.be (K. Maes), ileana.calotescu@utcb.ro (I. Calotescu), geert.lombaert@kuleuven.be (G. Lombaert), repetto@dicca.unige.it (M.P. Repetto).

https://doi.org/10.1016/j.jweia.2026.106436
Received 18 September 2025; Received in revised form 12 March 2026; Accepted 24 March 2026

through full-scale monitoring is very rare in the literature. Ballio et al. (1992) studied the wind response of a 100 m tall lattice tower built in 1933 using analytical methods and full-scale vibration monitoring. They reported a damping ratio of the fundamental mode obtained from operational modal analysis in the range of 0.3%–0.5%. Glanville et al. (1996) studied the first mode of vibration damping ratios of 67 m and 233 m tall lattice towers using forced vibration testing and found them to be in the range of 0.7%–1%. Shanmugasundaram et al. (1999) calculated the damping ratio of the fundamental mode for a 53 m tall lattice tower using ambient vibration data and found it to be in the range of 1.6%–2.6%. García et al. (2021) studied the dynamic properties of a 50 m tall lattice tower using operational modal analysis and found the damping ratios of the first five modes to be in the range of 0.21 to 0.27%.

Aerodynamic damping of lattice towers has not been extensively investigated through full-scale vibration monitoring because it requires long-term simultaneous measurement of structural vibration and wind speed. Glanville et al. (1996) reported that the first mode damping, obtained from ambient vibration data using the random decrement method and the autocorrelation methods, depends strongly on the mean wind speed, although a clear increasing or decreasing trend is not observed. Shanmugasundaram et al. (1999) found that the first mode damping, estimated from ambient vibration data using the half-band power method, increased with mean wind speed, indicating a positive contribution from aerodynamic damping. More recently, Azzi et al. (2021) evaluated the first mode alongwind and crosswind aerodynamic damping from vibration measurements of a scaled aeroelastic model tested in a wind tunnel. Their result showed that aerodynamic damping in the alongwind direction increases with the mean wind speed, consistent with the one calculated using the quasi-steady theory, while the crosswind aerodynamic damping changed sign as wind speed increased.

Routine structural design against wind loads usually relies on damping ratios recommended in standards and codes. Eurocode 1-1-4 (2005) defines damping as a summation of structural damping, aerodynamic damping, and damping due to special devices. For steel lattice structures, it recommends a structural damping ratio of 0.3% for welded connections, 0.5% for high resistance bolt connections, and 0.8% for ordinary bolt connections. It also provides a formula for the aerodynamic damping of the fundamental bending mode in the alongwind direction, derived based on quasi-steady theory. The American Society of Civil Engineers standard, ASCE 7-05 (2005), recommends structural damping ratios between 0.15% and 0.5%. The international standard for wind actions on structures, ISO 4354 (2009), defines total damping as the summation of structural, aerodynamic, and additional damping provided by auxiliary damping devices. It recommends a structural damping ratio of 0.1% for steel lattice towers and provides a general formula for the calculation of aerodynamic damping according to quasi-steady theory. The variability between the recommended structural damping ratios in the standards calls for further investigation using full-scale monitoring vibration data.

The research presented in this paper uses long-term, full-scale vibration data of a 50 m tall self-supporting lattice tower to study the dynamic properties, as well as the aerodynamic damping and the time evolution of the dynamic properties. Over two years of high-frequency continuous vibration data were used to estimate the natural frequencies, mode shapes, and modal damping ratios of the 50 m tall self-supporting lattice tower. Aerodynamic damping and seasonal variability of the dynamic properties are investigated using the simultaneous measurements of vibration, temperature, and wind speed.

The monitored structure, the monitoring system, and the available data are described in Section 2. The system identification process and the results for a segment of data are presented in Section 3. The time evolution of the dynamic properties and aerodynamic damping is presented in Section 4. Finally, the conclusion and prospects are given in Section 5.

2. The monitored structure and measurement setup

The monitored structure is a 50 m tall self-supporting lattice tower located in Sannicolau Mare, Romania, that supports telecommunication antennas. The three-legged tower has V bracing for the lower sections and N bracing for the rest (Fig. 1). All the members of the tower are hollow circular cross-sections made of steel and are connected by high-strength bolts. The distance between the three legs of the tower is 7.5 m at the base, tapering linearly to 2.3 m at a height of 40 m. The legs are vertical from a height of 40 m to the top of the tower. The tower has a ladder at the center, two resting platforms at 15 m and 27 m, and two working platforms at 40 m and 47.5 m. The total mass of the structure is approximately 12.6 tons (Fig. 1).

The monitoring system consists of triaxial accelerometers on one of the legs at 27 m and 50 m, strain gauges on the three legs and three diagonals at the base, temperature measurement for the outside environment, and an ultrasonic anemometer at the top of the tower. Fig. 1 shows the sensor locations and the measurement directions for the two accelerometers. Reference axes X–Y, which are parallel and perpendicular to the sides of the base triangle, are also shown. Strain gauges SG-L1, SG-L2, and SG-L3 are attached to Leg 1, Leg 2, and Leg 3 of the tower, respectively. Strain gauges SG-D23, SG-D23, and SG-D23 are attached to the diagonal members of the tower. Accelerometers A-27 and A-50 are attached to Leg 2 of the tower, measuring accelerations at 27 m and 50 m in the X, Y, and Z directions. The temperature sensor and the anemometer are attached to Leg 1 of the tower at 50 m. The sampling frequency is 100 Hz for the accelerometers, strain gauges, and temperature sensor, and 4 Hz for the anemometer. Detailed geometrical properties of the monitored structure and further information on the monitoring system can be found in Calotescu et al. (2025).

The monitoring system has registered simultaneous measurements of wind speed, temperature, and structural response data since March 2021. About two years of data from July 2021 to June 2023 are considered for this study. Fig. 2 is a wind rose diagram showing the mean wind speed and direction averaged over 10 min, registered during the two years considered. The diverse intensities of wind speeds and wind directions during the considered period allowed us to study aerodynamic damping.

3. System identification

In this section, the system identification of the lattice tower using acceleration and strain data is explained. The dynamic properties obtained using the vibration record of August 08, 2022, are presented. Later, in Section 4, the results from two years of acceleration data are presented to investigate aerodynamic damping and the time evolution of dynamic properties.

The system identification to obtain the natural frequencies, mode shapes, and modal damping ratios was done using the MACEC 3.4 Matlab toolbox for experimental and operational modal analysis, developed at KU Leuven (Reynders et al., 2014). Initially, the acceleration and strain data were processed by removing the low-frequency components using a fifth-order Chebyshev Type I highpass filter with a cutoff frequency of 0.5 Hz. For computational efficiency, the signals were resampled with a decimation factor of 5, resulting in a new sampling frequency of 20 Hz. To avoid aliasing while resampling the signal, a digital eighth-order low-pass Chebychev Type I filter with a cutoff frequency of 8 Hz was applied in both the forward and reverse directions to remove all phase distortion before resampling the data.

Fig. 3 shows the power spectral density (PSD) of the filtered 24-hour acceleration and strain data, calculated using the Welch method (Welch, 1967) with 2^{14} points and 50% overlap. From the PSD of acceleration and strain, a clear peak can be observed at a frequency of about 1.7 Hz, and multiple peaks can be observed between 4 and 6 Hz. It should be noted that some of the peaks between 4 and 5 Hz are only visible in

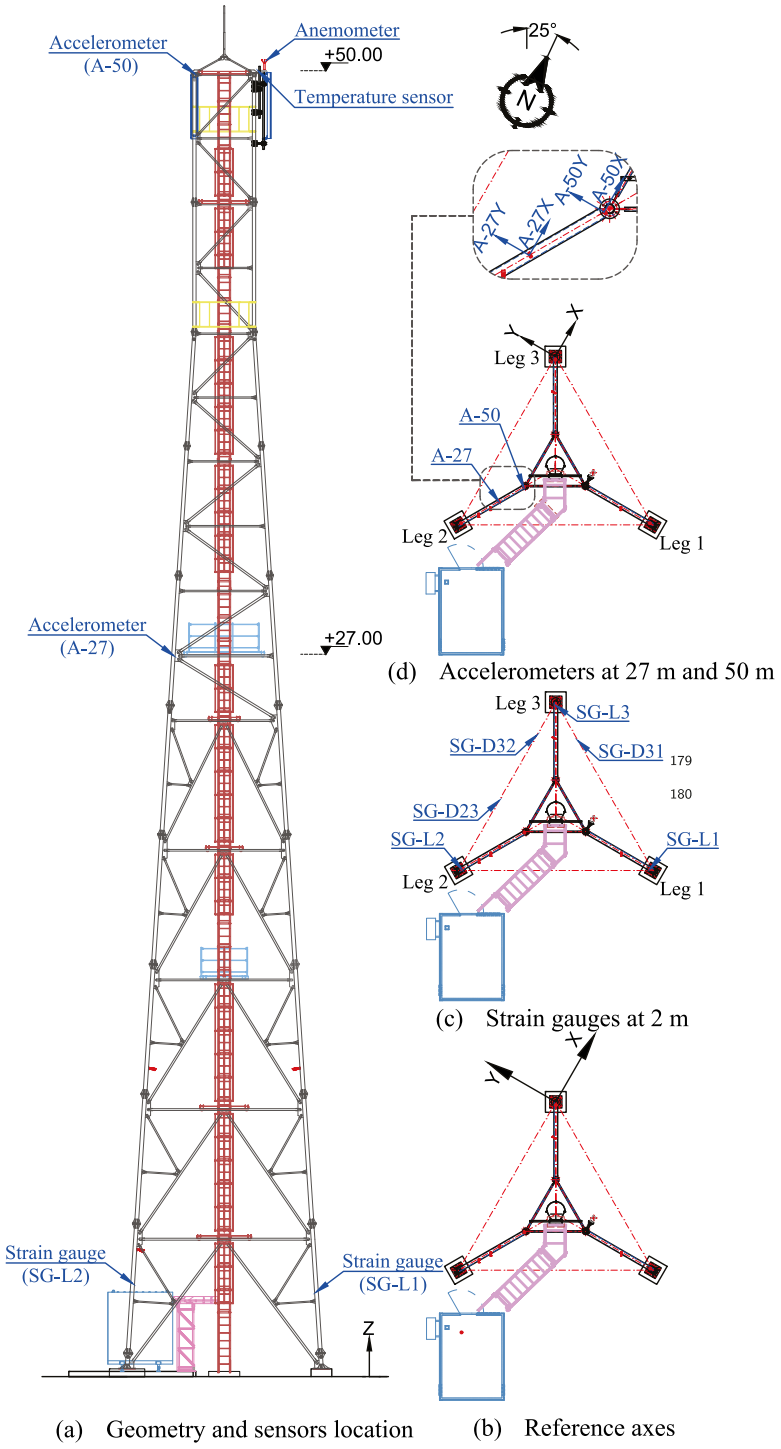

Fig. 1. Overview of the lattice tower and sensors' location.

the PSD of the three strain gauges attached to the diagonal members, not in the PSD of those attached to the legs of the tower.

The acceleration and strain data were processed using the reference-based covariance-driven stochastic subspace identification algorithm (SSI-cov/ref) to extract the modal properties. The half number of block rows in the correlation matrix is assigned a value $i = 100$. A model order ranging from 2 to 80 in increments of 2 is considered for the construction of the stabilization diagram. The acceleration data are adopted as a reference for data projection in the construction of the Toeplitz matrix (Peeters and Roeck, 1999). The modal properties, such as natural frequencies, modal damping ratios, and modal shapes, were extracted for the stable modes. Table 1 shows the modal properties for the first four modes obtained from operational modal analysis (OMA) through SSI-cov/ref and finite element model (FEM) analysis. Columns 2 and 9 list the natural frequencies while Column 3 reports the modal damping ratios. Columns 4 and 10 describe the mode shapes. Columns 5 to 7 provide the modal phase collinearity (MPC), mean phase of the mode shape (MP), and the mean phase deviation of the mode shape (MPD), which are used to evaluate the quality of the identified modes. For lightly damped structures, a good quality of identified modes is correlated with values of MPC, MP, and MPD closer to 1, 0°, and 0 °, respectively. The natural frequencies obtained from the full-scale

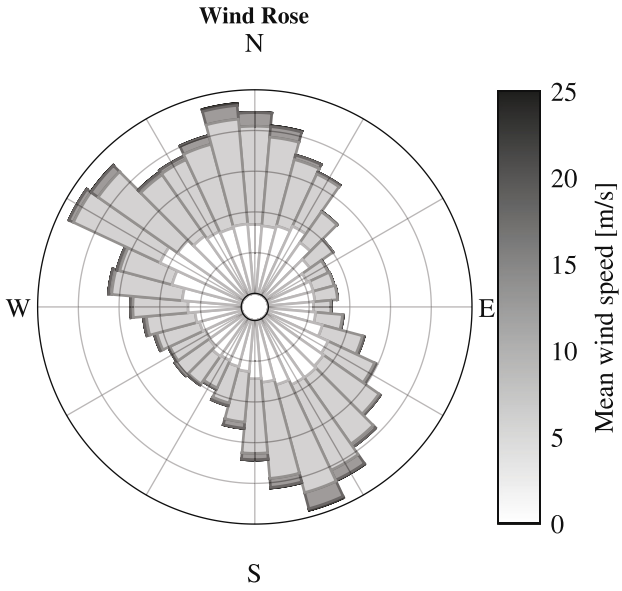

Fig. 2. Collected wind speed data.

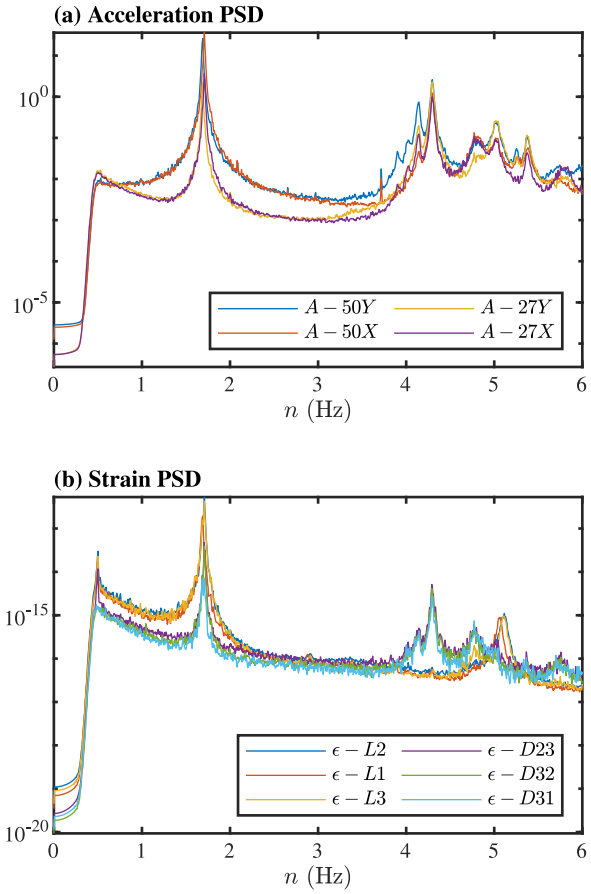

Fig. 3. PSD of strain and acceleration.

monitoring data and the FEM analysis are very close for the first and second modes and differ significantly for the third mode. The fourth mode, identified as torsional by the OMA, was not identified in the FEM analysis. Rather, the FEM analysis indicated that the fourth mode is a double-curvature bending about the Y-axis. The discrepancy between the two results primarily stems from the level of detail retained in the finite element model. The FEM detailed the geometry of the main three-legged tower structure while representing the ladders, platforms, and additional elements as masses. These resulted in the omission of additional stiffness components that are not symmetrically distributed and whose masses might not have been determined with sufficient accuracy. Further details on the FEM can be found in Calotescu et al. (2025).

Fig. 4 shows the corresponding strain and displacement mode shapes. The geometry is simplified with only a few elements to show the mode shape obtained using the limited number of sensors. The modal displacements at points where there are no response measurements were obtained using linear interpolation. The strain mode shapes were plotted using the mode shape information corresponding to the strain measurement on the three legs. The mode shape information from the strain measurement on the diagonal members was not used to plot the strain mode shapes because, out of the six diagonal members connected to the three legs at the base, only three had strain measurements.

Focusing on the displacement mode shapes, the first and second modes are first-order bending about the two orthogonal measurement directions, X and Y, respectively. The third and fourth mode shapes could not be easily identified from the displacement mode shapes because acceleration was measured on only one of the tower legs at two heights. However, as stated in the previous section, at the natural frequencies of these two modes, the PSD of the strain has peaks only for the diagonal bracing elements and not for the legs. Since torsional moment does not result in axial strain on the legs, this indicates that the third and fourth modes are torsional (Fig. 3).

The strain mode shapes are in agreement with the displacement mode shapes for the first two modes. For the third and fourth modes, the strain mode shapes are not clear because the strain gauges on the legs have no information about the two modes (there is no strain on the legs due to torsion).

The modal assurance criteria (MAC) value, which is a statistical indicator that measures the correlation and agreement between two sets of vibration mode shapes, was calculated between each of the mode shapes and plotted in Fig. 5 (Allemang, 2003). The MAC value between the first and second mode shapes is close to zero, indicating that they are orthogonal to each other.

4. Dynamic properties from long-term monitoring data

In this section, two years of monitoring data are used to study the modal properties of the structure, considering time evolution, temperature influence, and dependency on wind intensity.

4.1. Time evolution of the dynamic properties

The selected two years of data were divided into consecutive 1-hour segments. The mean wind speed, mean wind direction, and mean outside temperature were calculated for each 1-hour segment. Since the strain gauges did not result in reliable measurement data for most of the monitoring period, only the acceleration records at 27 m and 50 m for each 1-hr segment were used to investigate the dynamic properties. Similar to Section 3, the acceleration data were first high-pass filtered at 0.5 Hz, and the signal was resampled at a sampling frequency of 20 Hz with an appropriate prior low-pass filtering. Afterwards, the MACEC 3.4 MATLAB toolbox was used with an additional script to process several 1-hr data segments at once.

System identification using stochastic subspace identification typically requires selecting stable structural modes from a stabilization diagram. For a few recording segments, this selection can be done manually by visually inspecting the diagram. However, visual inspection becomes impractical when working with long-term vibration data divided into numerous hourly or daily segments. This study addressed the issue by applying a cyclic modal tracking approach that avoids

Table 1
Natural frequencies, n_j, modal damping ratios, ξ_j, MPC (modal phase collinearity), MP (mean phase), and MPD (mean phase deviation).

OMA							FEM		
Mode no.	n_j [Hz]	ξ_j [%]	Mode shape [–]	MPC [–]	MP [°]	MPD [°]	Mode no.	n_j [Hz]	Mode shape [–]
1	1.69	0.43	1st order bending (about X axis)	1.00	0.01	1.43	1	1.72	1st order bending (about X axis)
2	1.71	0.42	1st order bending (about Y axis)	1.00	−0.02	2.23	2	1.72	1st order bending (about Y axis)
3	4.14	0.64	Torsion	0.99	0.66	2.25	3	3.71	Torsion
4	4.30	0.36	Torsion	0.98	1.39	3.33	–	–	–

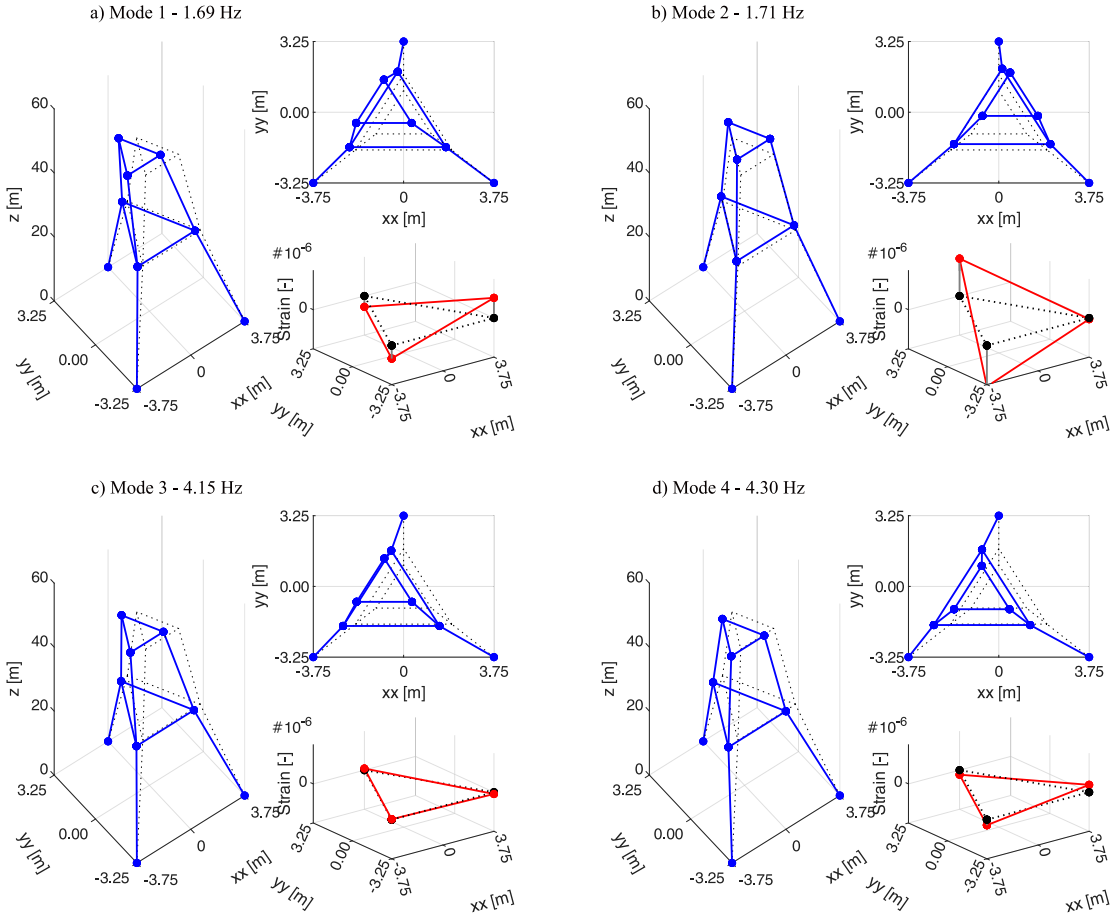

Fig. 4. Displacement and strain mode shapes.

manual inspection for each segment. Initially, stable modes were identified in one representative 1-hour segment through visual inspection using the MACEC GUI, and the corresponding natural frequencies were recorded as reference values. For each subsequent 1-hour segment, the natural frequencies were selected as the mean of the frequencies closest to the current reference values identified for all model orders. If the difference between the newly identified natural frequencies and the reference values exceeded a predefined threshold, the reference values were updated to the newly identified frequencies. This cycle was repeated sequentially across the entire two-year dataset to track seasonal variations in natural frequencies. The update thresholds were set to 0.01 Hz. This value was chosen because it produced clear seasonal trends and performed better than the tested lower and higher thresholds.

After analyzing all the consecutive data segments, outliers, defined as those that are more than 1.5 interquartile ranges above the upper quartile (75%) or below the lower quartile (25%), were removed from the obtained natural frequencies for each mode separately. The outliers for each mode constituted less than 2% of the results for all 1-hour data segments in two years. Damping ratios and mode shapes associated with the detected outliers in the natural frequencies have also been removed. Fig. 6 shows the time evolution of the natural frequencies after removing outliers. The seasonal variability in the modal vibration frequencies can be observed. The natural frequencies appear to be higher during the winter months and lower during the summer months. It should be noted that the range of the frequency axis in Fig. 6 is very small, and the modal frequency variability does not exceed 2%. Similar day and night variations, not included in this paper for brevity, were observed.

To investigate the extent of correlation of the natural frequencies with the outside temperature, the natural frequencies of the first four modes were plotted against the mean outside temperature averaged over 1 h in Fig. 7. The correlation was modeled through a first-order polynomial using linear regression analysis, and the best-fitting line is shown in black. The natural frequencies decrease by 0.003 to 0.01 Hz for a 10 °C increase in temperature. The variation might be small to significantly affect the wind-induced dynamic response of the structure, but it is important to be considered in structural health monitoring to avoid a false indication of damage.

Fig. 8 shows the time evolution of the total damping ratios of the first four modes. Adopting a similar definition for outliers as defined for

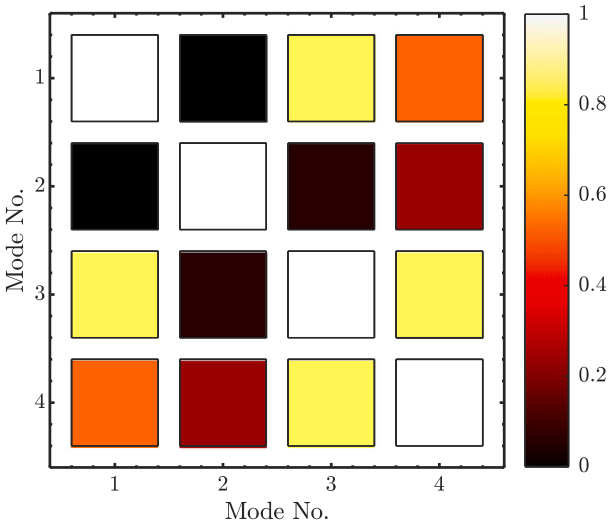

Fig. 5. MAC value.

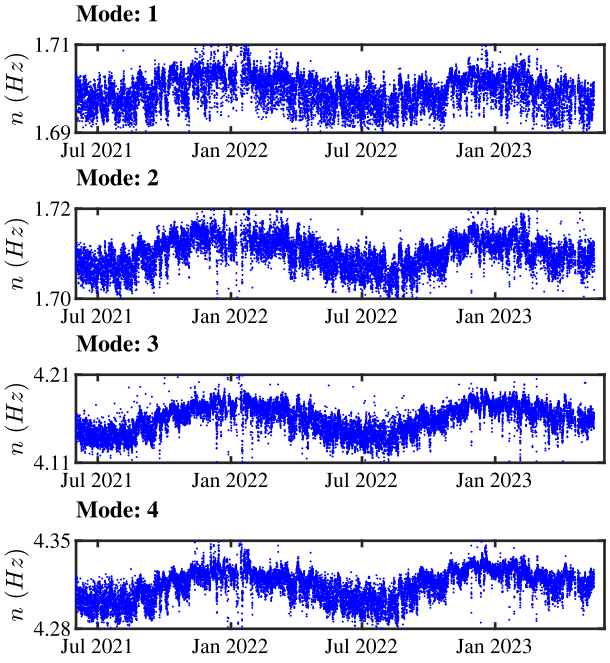

Fig. 6. Natural frequency.

the natural frequencies, outliers in the damping ratios for each mode were removed. The total number of outliers comprises less than 3.5% of the total data points. The damping ratios of the first four modes were obtained with a small variability. Although not included in this paper for brevity, a slight dependency of the damping ratio on temperature was observed for the torsional modes (modes 3 and 4).

Since design against wind usually considers the first bending modes in the orthogonal directions, the distribution of the total damping ratios of the first bending modes has been further studied by plotting their distribution through a histogram, as shown in Fig. 9. The total damping ratios for both modes are less than 0.6%. This value agrees closely with the recommendation for the structural damping ratio given in ASCE 7-05 (2005) (0.15%–0.5%); however, the recommended structural damping ratio in Eurocode 1-1-4 (2005) (0.5%) appears to be on the higher end of the damping distribution in Fig. 9. From

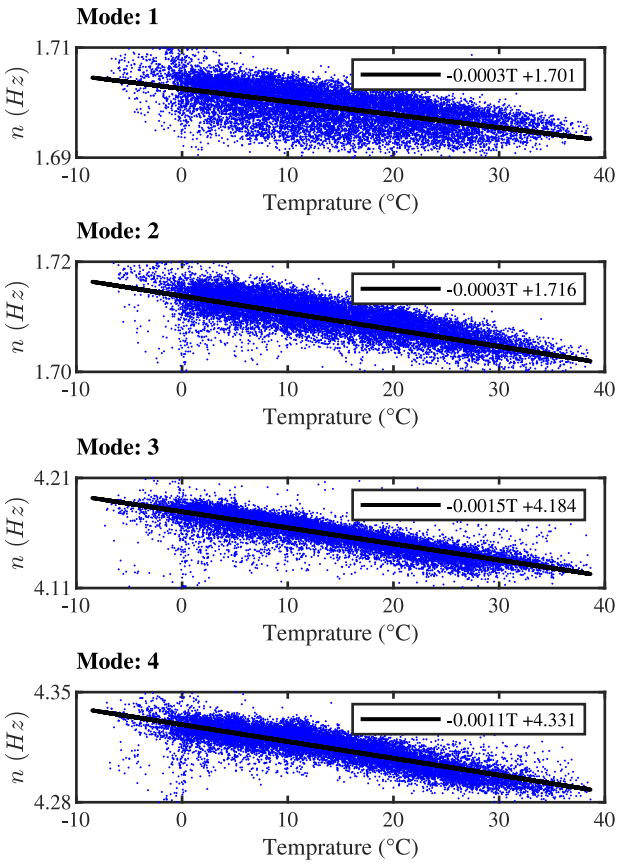

Fig. 7. Variation of natural frequency with outside temperature.

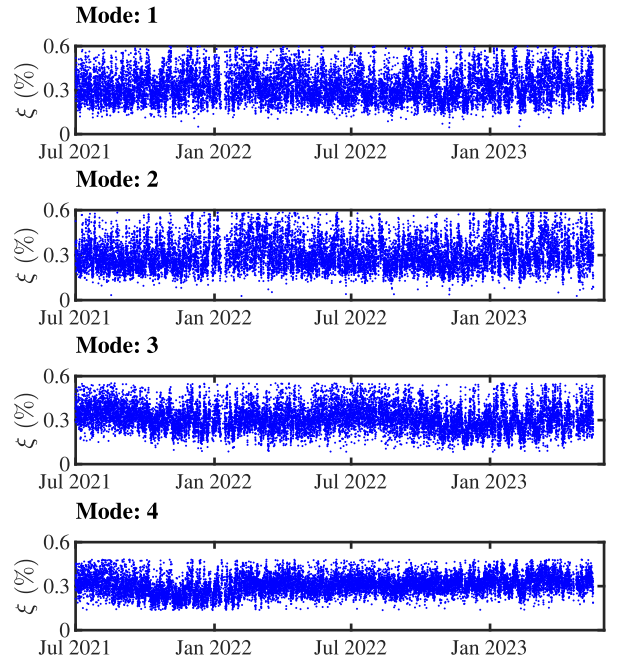

Fig. 8. Total damping ratio.

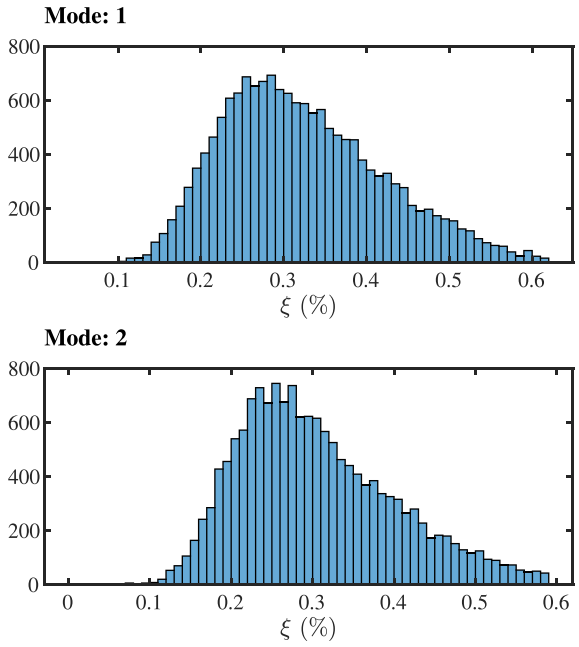

Fig. 9. Total damping ratio.

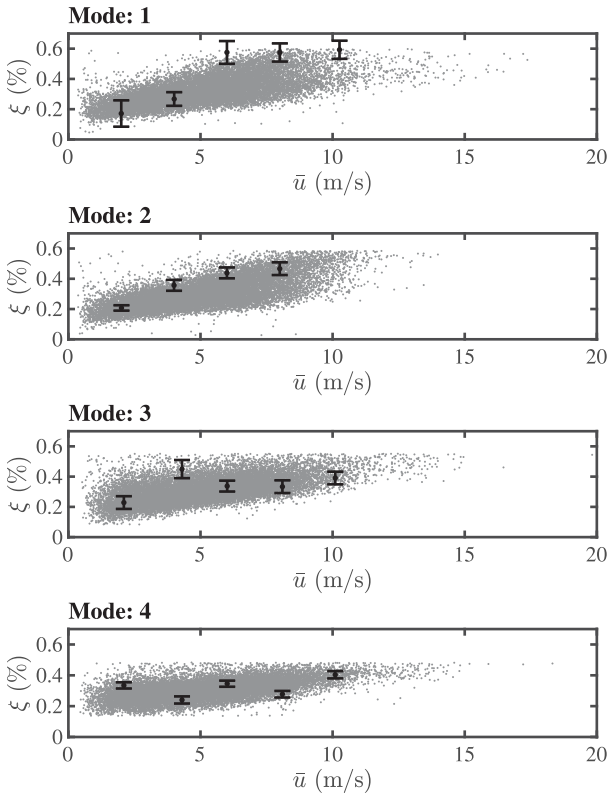

Fig. 10. Effect of wind speed on the total damping ratio. Error bars indicate $+/-3\sigma$ of the estimated damping ratios for five data points.

the histogram, it can also be observed that the recommended structural damping ratio in ISO 4354, 0.1%, is on the lower end of the distribution (ISO 4354, 2009).

4.2. Damping as a function of wind speed

Damping can vary with wind speed due to aerodynamic effects, amplitude-dependent structural damping, soil–structure interaction, vortex-induced vibration, and other sources. Aerodynamic damping is a parameter that can significantly contribute to the overall damping in slender structures excited by wind. However, its investigation is usually limited to wind tunnel testing, probably because of the scarcity of long-term full-scale data with simultaneous recording of wind speed and structural response.

Fig. 10 shows the total damping ratio versus mean wind speed for the first four modes. First, it can be observed that the damping ratios do not extend beyond a certain value for each mode, and this is because values above a certain threshold were detected as outliers, which are less than 3.5% of the total data points, as explained in the previous section. Second, a clear increase in the damping ratio with the mean wind speed can be observed for all four modes. The modal damping ratio increases from approximately 0.2% at low wind speeds to 0.6% at higher wind speeds. This is evident for all four considered modes. This increase in the damping ratio with the mean wind speed can be attributed to aerodynamic damping. However, other effects, such as amplitude-dependent structural damping and soil–structure interaction, might have also contributed to it. Identifying the exact cause of the increase in damping with the wind speed is not straightforward, as it is difficult to separate the effects of the different damping mechanisms in the test. While it is difficult to decouple effects contributing to damping from full-scale structure vibration data analysis, forced vibration experiments on scaled models in wind tunnels can be explored to separate the contributions of different damping mechanisms from the total damping.

Although the results in Fig. 10 show a clear trend with an overall increase of the modal damping ratios with wind speed, it cannot be neglected that the data are characterized by relatively large scatter. For a given wind speed, the damping ratios in Fig. 10 typically show a variation of about 0.1% with respect to the mean value. This variation has two potential sources. First, noise on the acceleration data in combination with a lack of knowledge on the excitation of the mast leads to estimation uncertainty in the modal analysis. Second, apart from the clear influence of wind speed, it is very likely that other environmental variables affect structural damping. One could, for example, expect that the soil stiffness at the support of the mast shows an influence of temperature as well as the level of the groundwater table. To separate both effects, the estimation uncertainty of the modal damping ratio estimates has been quantified using SSI-cov for five data points corresponding to different wind speeds. The resulting $+/-3\sigma$ uncertainty interval for these five data points is shown in Fig. 10 using error bars. The scatter in the damping ratio estimates exceeds the bounds of the estimation uncertainty indicated by the error bars.

Pagnini et al. (2025) assessed the damping ratios of monopole steel structures through full-scale monitoring and emphasized the need to consider different damping ratios for vortex-induced vibration (VIV), fatigue assessment, and design against gust buffeting vibration. For slender structures, VIV typically occurs at lower and more frequent wind speeds, and similarly, fatigue results from the most frequent vibrations associated with lower wind speeds. Therefore, damping ratios associated with lower wind speeds are most appropriate for design against VIV and fatigue. In contrast, gust buffeting vibration is assessed for the design wind speed, mostly above 20 m/s, so damping ratios associated with higher wind speeds can be used. For lattice structures similar to the one studied in this paper, an overall damping ratio of approximately 0.2% may be appropriate for assessing fatigue, whereas a value around 0.5% may be more suitable for gust buffeting analysis.

Eurocode 1-1-4 (2005) and the International standard for wind actions for structures, ISO 4354 (2009), define total damping as the summation of structural damping, aerodynamic damping, and damping due to special devices. A general definition of alongwind aerodynamic damping based on quasi-steady theory is given in both standards. Aerodynamic damping in the alongwind direction for lattice towers

with the assumption of quasi-steady theory is given by Holmes (1996):

$$\xi_{a1} = \frac{\rho \int_0^h \delta(z)\bar{u}(z)b(z)c_f(z)\psi_1^2(z)dz}{4\pi n_1 \int_0^h m(z)\psi_1^2(z)dz} \quad (1)$$

where ρ is the air density; $\delta(z)$ is the solidity ratio defined as the ratio between the total projected area and the projected envelope area perpendicular to the wind direction; $\bar{u}(z)$ is mean wind speed; $b(z)$ is the reference width of the cross-section, c_f is the force coefficient; $m(z)$ is the mass per unit length; n_1 is the first mode natural frequency and ψ_1 is the first mode shape.

The alongwind aerodynamic damping ratio in the first bending directions X and Y was calculated using Eq. (1) for different wind speed intensities. The considered parameters are, air density $\rho = 1.225$ kg/m^3; solidity ratio $\delta(z)$ calculated for the projected area perpendicular to X and Y directions; mean wind speed following the logarithmic vertical profile with a roughness height $z_0 = 0.05$ m; reference width $b(z)$ measured perpendicular to the X and Y directions; force coefficient $c_f = 1.4$ according to Eurocode 1-1-4 (2005); mass per unit length, $m(z)$, varying with height; $n_1 = 1.7$ Hz; and first mode shape in the X and Y direction modeled as $(z/50)^{1.92}$ obtained from the mode shape identification.

The structural damping ratios in the X and Y directions, ξ_s, were calculated from the full-scale result (Fig. 10), retaining only the damping ratios obtained with mean wind speeds less than 2 m/s and calculating the mean. The structural damping ratios in the X and Y directions were found to be 0.23% and 0.24%, respectively. These values are much lower than the structural damping ratio recommended in Eurocode 1-1-4 (2005) (0.5%) and slightly higher than the recommended structural damping ratio in ISO 4354 (2009)(0.1%). This indicates that the total damping calculated as the sum of structural and aerodynamic damping according to Eurocode 1-1-4 (2005) will be much higher than the total damping obtained from the full-scale vibration data analysis. The overestimation would have been even higher if amplitude-dependent structural damping and other mechanisms were part of the total damping calculation.

The total damping ratios in the X and Y directions were calculated as the sum of the structural damping ratios, ξ_s, obtained using the full-scale monitoring data and the aerodynamic damping ratios obtained using quasi-steady theory (Eq. (1)). To make a direct comparison between the calculated total damping ratio and the result of full-scale vibration monitoring, only data corresponding to wind along the X and Y directions (±10°) were selected from the full-scale vibration data. This was necessary because aerodynamic damping in Eq. (1) is derived assuming that the alongwind direction coincides with the first mode bending directions, X and Y. Thus, from the first and second mode damping ratios shown in Fig. 10, only those corresponding to wind along the X and Y directions are selected. Recall that the first mode of vibration of the monitored structure is bending in the Y direction, while the second mode of vibration is bending in the X direction. For wind along the Y axis, the first mode damping ratio is the damping ratio in the alongwind direction, while the second mode damping ratio is the damping ratio in the crosswind direction. Similarly, for wind along the X axis, the second mode damping ratio is the damping ratio in the alongwind direction, while the first mode damping ratio is the damping ratio in the crosswind direction.

Fig. 11 shows the total damping ratio obtained using the full-scale monitoring data in the alongwind and crosswind directions when the mean wind direction is along the X and Y axes, with a threshold of ±10°. The structural damping ratio, ξ_s, obtained from the full-scale vibration data is shown with a horizontal dashed line. The total damping in the alongwind direction, calculated as the sum of the aerodynamic damping from quasi-steady theory (Eq. (1)) and structural damping, ξ_s, obtained from the full-scale vibration data, is also shown with a solid black line. In general, the total damping ratio increased with the mean wind speed, both in the alongwind and in the crosswind directions. The

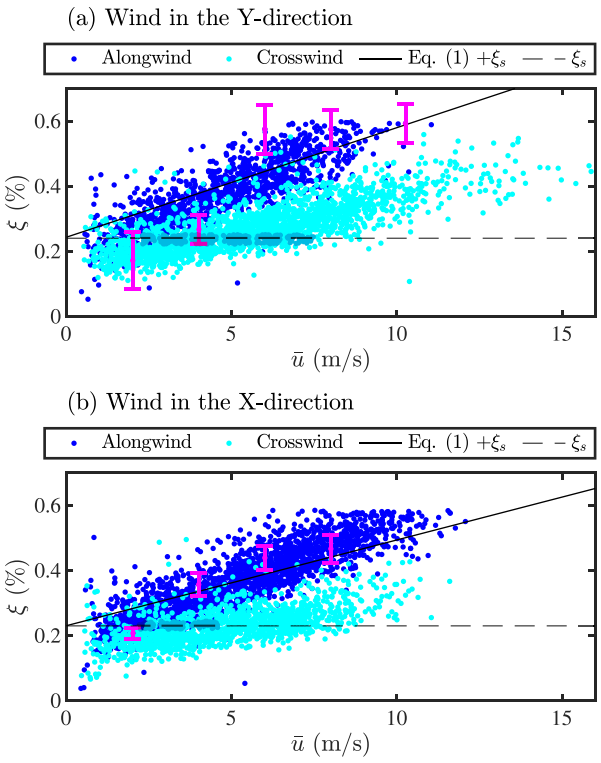

Fig. 11. First mode damping in the alongwind and crosswind direction. Error bars indicate +/−3σ of the estimated damping ratios for five data points.

increasing trend of the alongwind damping obtained from the full-scale vibration is closely similar to the one obtained using the quasi-steady theory (Eq. (1)). Although damping in the crosswind direction is lower than that in the alongwind direction, it still increases with wind speed. In general, crosswind aerodynamic damping for slender structures can be negative for some angle of attack, resulting in a total damping that decreases with increasing wind speed (Kareem, 1978). Significant global vortex-induced vibration of self-supporting lattice towers is generally not likely because of their geometry. However, in the study of a self-supporting lattice tower using a scaled aero-elastic model by Azzi et al. (2021), the crosswind aerodynamic damping decreased with increasing mean wind speed for certain angles of attack. This was not evident from the results of the full-scale vibration data for the monitored lattice tower.

Similar to Fig. 10, Fig. 11 also shows the damping estimation uncertainty using error bars for five data points corresponding to different wind speeds. Unlike Fig. 10, the five data points in Fig. 11 correspond to wind along the Y direction (subplot (a)) and along the X direction (subplot (b)) with an additional threshold of ±10°. This separates the effect of wind direction on the scatter observed in Fig. 10 from the damping estimation uncertainty. In comparison to the previous plot, the scatter in the alongwind damping ratio in the Y-direction is mostly within the bounds of the estimation uncertainty shown by the error bars. The scatter in the alongwind damping ratio in the X-direction is also closer to the bounds of the estimation uncertainty relative to Fig. 10. This indicates that the scatter in the damping ratio estimation is mostly due to the damping estimation uncertainty instead of other environmental effects.

5. Conclusion

The dynamic properties of a 50 m tall, three-legged, self-supporting lattice tower were investigated using full-scale monitoring data. The natural frequencies, damping ratios, and mode shapes were determined

using ambient vibration data obtained using strain gauges and accelerometers. The Covariant-based stochastic subspace identification method was applied using the MACEC 3.4 Matlab toolbox for experimental and operational modal analysis. Two years of continuous vibration, temperature, and wind speed monitoring data were used to study the seasonal variation of the dynamic properties and the correlation between the damping ratio and mean wind speed.

The first two modes of vibration were found to be single curvature bending along two perpendicular directions at a frequency of ≈1.7 Hz. The natural frequencies have shown correlation with temperature, decreasing by 0.003–0.01 Hz for a 10 °C increase in temperature. Although the range of the variability in the natural frequencies with temperature might not significantly affect the dynamic response, it is important to consider it in structural health monitoring and online damage identification.

The total damping ratios of the first four modes were in the range of ≈0.1–0.6%. These values agree closely with the recommendation for structural damping ratio given in ASCE 7-05 (2005) (0.15–0.5%), while the recommendations given in Eurocode 1-1-4 (2005) (0.5%) and ISO 4354 (0.1%) are respectively on the higher and lower range of the obtained damping ratios. The damping ratios were highly correlated with the mean wind speed, increasing from ≈0.2% at low wind speeds to ≈0.6% at a mean wind speed of about 15 m/s. Defining the structural damping as that corresponding to lower wind speed (<2 m/s), it was shown that the structural damping ratio recommended in Eurocode 1-1-4 (2005) is significantly higher than that obtained from the full-scale vibration data analysis. This is particularly important considering that the total damping according to Eurocode 1-1-4 (2005) is the summation of the structural and aerodynamic damping. The damping ratio was further investigated by selecting data corresponding to wind directed along the first bending modes. Damping ratio increased with the mean wind speed in both the alongwind and crosswind directions. The increasing trend of aerodynamic damping in the alongwind direction, calculated using a quasi-steady based formulation, with the mean wind speed, was closely similar to that of the full-scale monitoring result.

The presented study is a valuable addition to the limited number of investigations into the dynamic properties of lattice towers based on full-scale measurements, especially on their damping properties. The long-term vibration data, collected over two years, enabled a comprehensive investigation of the damping ratio, a parameter often subject to significant uncertainty when studied with only a few full-scale measurement data. The study also emphasizes the importance of coupling vibration measurement sensors with meteorological sensors, such as anemometers and temperature sensors, to examine seasonal and wind-influenced variations in the dynamic properties.

CRediT authorship contribution statement

Mekdes T. Mengistu: Writing – original draft, Visualization, Investigation, Funding acquisition, Formal analysis, Data curation, Conceptualization. **Kristof Maes:** Writing – review & editing, Validation, Resources, Methodology, Conceptualization. **Ileana Calotescu:** Writing – review & editing, Software, Resources, Project administration, Funding acquisition, Data curation. **Geert Lombaert:** Writing – review & editing, Supervision, Software, Resources, Methodology, Conceptualization. **Maria Pia Repetto:** Writing – review & editing, Supervision, Resources, Project administration, Funding acquisition, Conceptualization.

Declaration of competing interest

The authors declare that they have no known competing financial interests or personal relationships that could have appeared to influence the work reported in this paper.

Acknowledgments

The full-scale structural monitoring system was supported by a grant from the European Research Council (ERC) under the European Union's Horizon 2020 research and innovation program (grant agreement No. 741273) for the project "THUNDERR - Detection, simulation, modeling and loading of thunderstorm outflows to design wind-safer and cost-efficient structures" – through an Advanced Grant 2016. The participation of the first author was supported by a grant for a scientific stay in Flanders (grant ID V507724N) by the Research Foundation Flanders (FWO), Belgium.

Data availability

Data will be made available on request.

References

Allemang, R.J., 2003. The modal assurance criterion - Twenty years of use and abuse. Sound Vib. 14–21.
ASCE 7-05, 2005. Minimum design loads for buildings and other structures. p. 419,
Augusti, G., Bartoli, G., Borri, C., Gusella, V., Spinelli, P., 1992. Wind load and response of broadcasting antennas: three years of research work in cooperation with RAI. J. Wind Eng. Ind. Aerodyn..
Azzi, Z., Elawady, A., Irwin, P., Chowdhury, A.G., Shdid, C.A., 2021. Aeroelastic modeling to study the wind-induced response of a self-supported lattice tower. Eng. Struct. 245, 112885. http://dx.doi.org/10.1016/j.engstruct.2021.112885.
Ballio, G., Maberini, F., Solari, G., 1992. A 60 year old, 100 m high steel tower: limit states under wind actions. J. Wind Eng. Ind. Aerodyn. 2089–2100.
Calotescu, I., Bîtcă, D., Repetto, M.P., 2025. Full-scale monitoring of a telecommunication lattice tower under synoptic and thunderstorm winds. J. Wind Eng. Ind. Aerodyn. 258, http://dx.doi.org/10.1016/j.jweia.2025.106022.
Calotescu, I., Solari, G., 2016. Alongwind load effects on free-standing lattice towers. J. Wind Eng. Ind. Aerodyn. 155, 182–196. http://dx.doi.org/10.1016/J.JWEIA.2016.06.004.
Eurocode 1-1-4, 2005. Eurocode 1: Actions on structures-part 1-4: General actions-wind actions.
García, K.L., Maes, K., Parnás, V.E., Lombaert, G., 2021. Operational modal analysis of a self-supporting antenna mast. J. Wind Eng. Ind. Aerodyn. 209, http://dx.doi.org/10.1016/j.jweia.2020.104490.
Glanville, M.J., Kwok, K.C., Denoon, R.O., 1996. Full-scale damping measurements of structures in Australia. J. Wind Eng. Ind. Aerodyn. 59, 349–364. http://dx.doi.org/10.1016/0167-6105(96)00016-5.
Haritos, N., Stevens, L., 1983. The assessment of response of tall free-standing towers to along-wind loading. J. Wind Eng. Ind. Aerodyn. 331–344.
Hiramatsu, K., Akagi, H., 1988. The response of latticed steel towers due to the action of wind. J. Wind Eng. Ind. Aerodyn. 30, 7–16. http://dx.doi.org/10.1016/0167-6105(88)90066-9.
Holmes, J.D., 1996. Along-wind response of lattice towers II. Aerodynamic damping and deflections. Eng. Struct. 18, 483–488. http://dx.doi.org/10.1016/0141-0296(95)00131-X.
Holmes, J.D., Schafer, B.L., Banks, R.W., 1992. Wind-induced vibration of a large broadcasting tower. J. Wind Eng. Ind. Aerodyn. 2101–2109. http://dx.doi.org/10.1016/0167-6105(92)90640-V.
Huang, P., Chen, S., Gu, M., 2019. Field measurement and aeroelastic wind tunnel test of wind-induced vibrations of lattice tower. Struct. Des. Tall Spec. Build. 28, http://dx.doi.org/10.1002/tal.1622.
ISO 4354, 2009. International standard: Wind actions on structures.
Kareem, A., 1978. Wind Excited Motion of Buildings (Ph.D. thesis). Colorado State University, Fort Collins, Colorado.
Pagnini, L., Orlando, A., Repetto, M.P., 2025. Damping assessment of monopole steel structures through full-scale experiments. Eng. Struct. 327, http://dx.doi.org/10.1016/j.engstruct.2025.119627.
Peeters, B., Roeck, G.D., 1999. Reference-based stochastic subspace identification for output-only modal analysis. Mech. Syst. Signal Process. 855–878. http://dx.doi.org/10.1006/mssp.1999.1249, URL http://www.idealibrary.comon.
Peng, H., Sheng, C., Xuanyi, Z., Gu, M., 2017. Aeroelastic model test and field measurement of 40-m high lattice tower. In: 9th Asia-Pacific Conference on Wind Engineering. Auckland, New Zealand.
Reynders, E., Schevenels, M., De Roeck, G., 2014. MACEC 3.3: A Matlab Toolbox for Experimental and Operational Modal Analysis. Department of Civil Engineering, KU Leuven.
Shanmugasundaram, J., Harikrishna, P., Gomathinayagam, S., Lakshmanan, N., 1999. Wind, terrain and structural damping characteristics under tropical cyclone conditions. Eng. Struct. 21, 1006–1014. http://dx.doi.org/10.1016/S0141-0296(98)00053-4.
Welch, P.D., 1967. The use of fast Fourier transform for the estimation of power spectra: A method based on time averaging over short, modified periodograms. IEEE Trans. Audio Electroacoust. 15, 70–73. http://dx.doi.org/10.1109/TAU.1967.1161901.